HEFAT2010
7th International Conference on Heat Transfer, Fluid Mechanics and Thermodynamics
19-21 July 2010
Antalya, Turkey

PROBABILISTIC FLOW REGIME CLASSIFICATION OF HORIZONTAL REFRIGERANT FLOW BASED ON CAPACITIVE VOID FRACTION MEASUREMENTS

Canière H.*, T'Joen C. and De Paepe M.
*Author for correspondence
Department of Flow, Heat and Combustion Mechanics, Ghent University - UGent,
St.-Pietersnieuwstraat 41, Gent, 9000, Belgium
E-mail: Hugo.Caniere@UGent.be and Michel.DePaepe@UGent.be

ABSTRACT

A capacitive void fraction sensor was developed to study the objectivity in flow pattern mapping of horizontal refrigerant two-phase flow in macro-scale tubes. Sensor signals were gathered with R410A and R134a in an 8mm I.D. smooth tube at a saturation temperature of 15°C in the mass velocity range of 200 to 500 kg/m²s and vapour quality range from 0 to 1 in steps of 0.025. A visual classification based on high speed camera images is made for comparison reasons. A statistical analysis of the sensor signals shows that the average, the variance and a high frequency contribution parameter are suitable for flow regime classification into slug flow, intermittent flow and annular flow by using a the fuzzy c-means clustering algorithm. This soft clustering algorithm perfectly predicts the slug/intermittent flow transition compared to our visual observations. The intermittent/annular flow transition is found at slightly higher vapour qualities for R410A compared to the prediction of [Barbieri et al., 2008, Flow patterns in convective boiling of refrigerant R-134a in smooth tubes of several diameters, 5th European Thermal-Sciences Conference, The Netherlands]. An excellent agreement was obtained with R134a. This intermittent/annular flow transition is very gradual. A probability approach can therefore better describe such a transition. The membership grades of the cluster algorithm can be interpreted as flow regime probabilities. Probabilistic flow pattern maps are presented for R410A and R134a in an 8mm I.D. tube.

NOMENCLATURE

AVG		Average
CPSD		Cumulative power spectral distribution
D	[m]	Inner tube diameter
Fr	[-]	Froude number
G	[kg/m²s]	Mass velocity
c_p	[J/kgK]	Specific heat capacity
H	[J/kgK]	Enthalpy
m	[kg/s]	Mass flow rate
M2		Variance
M3		Skewness
M4		Kurtosis
P		Flow regime probability
PDE		Probability density estimation
PSD		Power spectral density
T	[K]	Temperature
V	[V]	Voltage signal
x	[-]	Vapour quality
X_{tt}	[-]	Lockhart-Martinelli parameter

Greek symbols

Δ	Difference
σ	Standard deviation

Sub- and Superscripts

A	Annular flow
I	Intermittent flow
L	Liquid
PH	Preheater
R	Refrigerant
S	Slug flow
sat	Saturation
V	Vapour
2PH	Two-phase
*	Dimensionless

INTRODUCTION

Complex two-phase flow phenomena occur during the phase change of refrigerant from liquid to vapour and vice versa. To accurately predict the heat transfer and pressure drop, these flow phenomena should be incorporated in the design models for in-tube evaporators used in refrigeration and air-conditioning [1]. Traditionally, this is achieved by classifying two-phase flows into flow regimes and presenting them in flow pattern maps. Recently, Cheng et al. [2] published a comprehensive review on flow regimes and flow pattern maps. Most of the two-phase flow classifications are based on visualizations (with or without use of high speed cameras). But visual-only methods are inherently subjective. Cheng et al. [2] assign this as the main reason why flow pattern data from different researchers are often inconsistent for similar test

conditions. Objective methods can therefore contribute to more accurate flow pattern data.

Rather than purely classifying a flow into mutually exclusive regimes, the classification problem can also be approached by describing the flow as a combination of different flow regimes each with a certain probability. Nino et al. [3] introduced the probabilistic approach in multiport microchannels. Jassim et al. [4] obtained probabilistic two-phase flow data of R134a and R410A in single horizontal smooth, adiabatic tubes (diameters ranging from 1.74mm to 8mm I.D.) by using an automated image recognition technique. Jassim [5] also developed curve fits for this time fraction data, which were used by Jassim et al. [6] for void fraction modeling and by Jassim et al. [7] for heat transfer modeling during condensation. However, so far it is not known how general such time fraction curve fits are [2].

This study aims to find more objectivity in flow pattern mapping. Therefore a capacitance probe was developed [8,9] as well as a transducer suitable for use with low dielectric fluids such as refrigerants [10]. The use of a signal clustering technique was previously investigated for air-water flows [11] and is now further studied for use with evaporating refrigerant flows to objectively and probabilistically describe flow regime transitions.

EXPERIMENTAL FACILITY

Refrigerant test facility

In Figure 1, a schematic of the refrigerant test facility is shown. A pump provides subcooled refrigerant to the preheater. This preheater consist of six tube-in-tube heat exchangers with a total length of 15m. The length of the preheater can be altered between 1m and 15m in steps of 1m. The refrigerant in the central tube is heated and evaporated to the desired vapour quality x, by hot water flowing in the annuli. A boiler system heats a 2m³ tank to provide hot water at a stable temperature during the experiments. The conditioned vapour-liquid mixture is fed into the test sections after which it is condensed back to liquid in a plate condenser. The condenser transfers the heat from the refrigerant to a water/glycol (30%) flow and provides subcooled liquid to the pump. The water/glycol mixture is supplied from a 1m³ tank which is cooled by a chiller system. In contrast with a traditional compressor loop, there is only one working pressure. The pump only bridges the pressure losses. By controlling the frequency of the pump the mass velocity G, in the refrigerant loop is set. The loop is connected to a reservoir which is submerged in a water bath. By changing the bath temperature, the saturation pressure in the loop can be altered.

The mass flow rate of the refrigerant as well as the mass flow rate of the water in the preheater, are measured using coriolis type flow meters with an accuracy of ±0.2% (of reading). Temperature measurements are performed using thermocouples (type K) which are insitu calibrated with an uncertainty of ±0.05°C. From these measurements, the heat balance of the preheater is determined (Eq. (1)). The uncertainty in this heat balance is monitored online. The vapour quality at the inlet of the test section is calculated using Eqs. (1) and (2).

$$m_R\left(h_{R,PHout} - h_{R,PHin}\right) = m_{w,PH}\, c_{p,w}\left(T_{w,PHin} - T_{w,PHout}\right) \quad (1)$$

$$x_{PH} = \frac{h_{R,PHout} - h_{R,L}}{h_{R,V} - h_{R,L}} \quad (2)$$

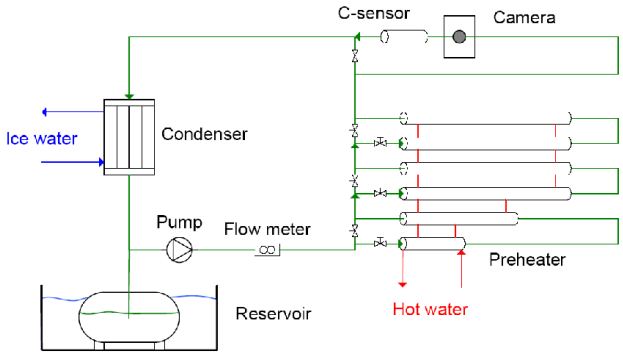

Figure 1 Schematic of refrigerant test facility

Adiabatic test section

A horizontal adiabatic test section is used for flow visualization and characterization purposes. It consists of a sight glass with a camera, the capacitive void fraction sensor and a second sight glass. To eliminate disturbances from bends or valves, a minimum entrance and exit length of 60D was ensured upstream and downstream of the test section. In that case, the flow in the test section is fully developed. A constant tube diameter is assured over the full length of the test section with as little disturbances as possible. To capture images of the refrigerant flow, a monochromatic high speed camera was used which could capture images at 250 frames per second.

Capacitive void fraction sensor

A capacitance probe with a concave electrode configuration was developed for dynamic two-phase flow void fraction measurements [8,12]. Capacitance probes use the difference in dielectric constant between the liquid phase and the vapour phase. The output of the probe is a voltage signal proportional to the capacitance of the two-phase mixture between the electrodes. To acquire (quasi)-local two-phase flow data, the electrode width is equal to the diameter of the tube.

The electronic transducer measures the capacitance between the electrodes at 2MHz and is based on the charge-discharge principle [10,12]. The electric current that flows because of this charging and discharging is converted to a voltage signal. These voltage signals are gathered at a sample frequency of 1kHz by the DAQ system and are made dimensionless according to Eq. (3). V_L and V_V are the voltage levels of liquid only and vapour only flowing in the tube.

$$V^* = \frac{V_{2PH} - V_V}{V_L - V_V} \quad (3)$$

The sensitivity of the transducer is 1.16V/pF. At 15°C, the difference between V_L and V_V was measured ΔV=1.32V for

R410A and ΔV=1.31V for R134a. The difference in electric capacitance between liquid flow and vapour flow is thus 1.14pF and 1.13pF respectively. The noise level of both liquid only and vapour only flow is 10mV (peak to peak). The corresponding uncertainty evaluated as 2σ is ±4mV or ±0.3% of ΔV, resulting in signal-to-noise ratios SNR higher than 300. The step response of the transducer to a change in capacitance of 1pF was faster than the sample frequency (1kHz).

EXPERIMENTAL RESULTS

Dataset and visual classification

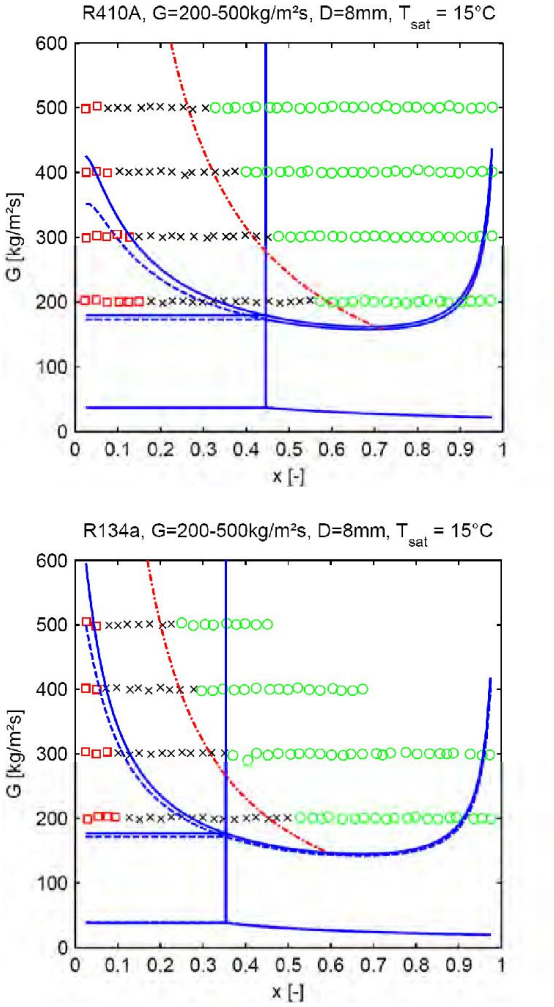

Figure 2 Wojtan-Ursenbacher-Thome flow pattern map (– – G=200 kg/m^{2}s, — G=500 kg/m^{2}s) under adiabatic conditions, Barbieri et al. I/A transition (-·-) with our visual classification (□ slug flow, x intermittent flow, o annular flow)

Capacitance sensor signals are gathered for R410A at T_{sat}=15°C. Four data series at mass velocities ranging from G=200 to 500 kg/m^{2}s are obtained with vapour qualities ranging from 0 to 1 in steps of 0.025. A similar set was gathered with R134a. But the G=400 kg/m²s and G=500 kg/m²s series are not complete up to x=1. Because of the larger pressure drop of R134a, the saturation temperature could not be kept constant at 15°C. In Figure 2, the dataset with our visual classification is shown in a Wojtan-Ursenbacher-Thome flowmap [13] under adiabatic conditions. Additionally the intermittent/annular flow transition of Barbieri et al. [14] is depicted as well (Eq. (4)).

$$G_{I-A}^2 = 3.75gD\frac{(1-x)^{0.16}}{x^{2.16}}\frac{\rho_V^{1.2}}{\rho_L^{-0.8}}\left(\frac{\mu_L}{\mu_V}\right)^{0.24} \quad (4)$$

Using the high speed camera images, the observed two-phase flows were classified into slug flow, intermittent flow and annular flow. The liquid slugs have to fill the entire tube but can be aerated to be classified as slug flow. In annular flow, the motion of the liquid flowing at the top of the tube should be comparable to the motion of liquid flowing at the bottom. Intermittent flow groups the remaining two-phase flows.

The slug flow/intermittent flow transition lines have the same trend but do not fully agree with our visual classification. This discrepancy can be partially due to the classification criterion.

In the flow pattern map of Wojtan et al. [13] the intermittent-annular flow transition is defined at a constant value of the Lockhart-Martinelli parameter X_{tt}=0.34. Thus, only density and viscosity are taken into account, resulting in a transition line at constant vapour quality. However, Barbieri et al. [14] concluded from their visual observations that this transition is also affected by tube diameter, mass velocity and vapour quality. They proposed a transition line as a function of the liquid Froude number and X_{tt} based on observations of R134a two-phase flows in smooth tubes with internal diameters varying from 6.2mm to 12.6 mm at T_{sat}=5°C, namely $Fr_L = 3.75X_{tt}^{2.4}$. Their transition line in G-x format (Eq. (4)) is set out in dash-dot in Figure 3 and agrees much better with our visual observations compared to the transition of Wojtan et al. [13]. The Barbieri et al. [14] criterion for intermittent-annular flow transition is found to be valid for the conditions at T_{sat}=15°C and for use with R410A.

Capacitive void fraction signals

Three typical sensor signals are shown in Figure 3, i.e. a slug flow, an intermittent flow and an annular flow signal obtained with R410A at T_{sat}=15°C. At low vapour qualities slugs frequently fill the entire cross section with liquid. Each liquid slug causes a peak in the voltage signal that approaches V^* =1. This results in a high variance in the signal values. The slug frequencies dominate the frequency spectrum. The average signal values of slug flows are high due to the large liquid content. At transition from slug flow to intermittent flow, the vapour content in the slugs is that high, that the liquid bridges break up. The interfacial waves are more turbulent in the intermittent flow regime, causing liquid droplets to swing into the vapour phase and vapour bubbles to appear into the liquid phase. The two-phase flow becomes fully chaotic. This results in a higher frequency spectrum content at frequencies higher than 5Hz. The tube perimeter remains fully wetted. The amplitude of the wave patterns diminishes and the liquid content in the upper film increases gradually.

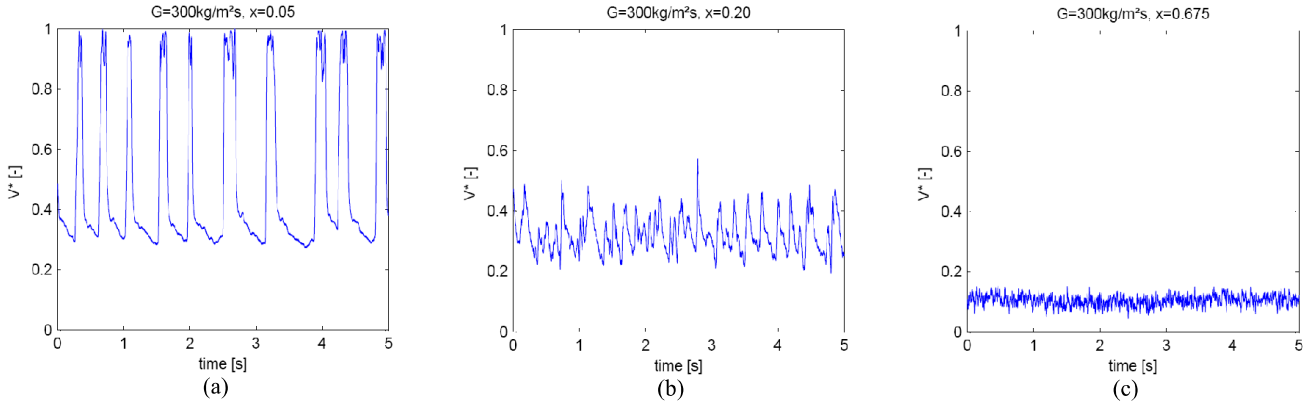

(a) (b) (c)

Figure 3 Capacitive void fraction signals of R410A at T_{sat} = 15°C slug flow (b) intermittent flow (c) annular flow

A further increase in vapour quality results in the development of an annular film. The thickness of the film always remains larger at the bottom of the tube. The transition from intermittent to annular flow is very gradual. In fully developed annular flow, the interface between the liquid annulus and the vapour core is disturbed by small amplitude waves. Droplets may be dispersed in the vapour core but these are hard to notice due to the limited visual access. The annular film thickness gradually diminishes with increasing x. The average signal values are low because of the high vapour content, the variance of the signal values is low as well, but the frequency content at high frequencies is high instead.

STATISTICAL ANALYSIS

From each signal of the dataset, several statistical features are mined which are investigated for their ability of flow regime classification. A first group consists of the statistical moments of the sensor signal, i.e. the average value (AVG), the variance (M2), the skewness (M3) and the kurtosis (M4). These features determine the shape of the probability density estimation (PDE) of a signal and represent information of the signal in the amplitude domain. A second group consists of features in the frequency domain, called F#-parameters. First, the power spectral density (PSD) was calculated using the fast Fourier algorithm. Then the cumulative distribution (CPSD) was taken of the PSD contributions between 0 and 100Hz. The features are then the frequencies corresponding to a certain percentile of this cumulative distribution. For example F50 is the frequency corresponding to the 50% percentile of the CPSD. This means that 50% of the power spectrum contribution (between 0-100Hz) is present in the frequencies lower than F50. The frequency range for vapour-liquid interface phenomena is typically smaller than 100Hz [15]. Therefore, only contributions of frequencies lower than 100Hz are considered. The purpose of the F#-parameters is to incorporate the effect of PSD contributions moving to higher frequencies and so track the intermittent-annular flow transition.

Several statistical tools were used to find the most suitable features for flow pattern detection. *Fisher Criterion tests* [16] as well as a *Principle component Analysis* (PCA) [17] were performed to the datasets of R410A and R134a. From this, the variance was found to have the highest potential in separating slug flows from non-slug flows. The AVG and F95 are most suitable for tracking the intermittent/annular flow transition. But in contrast with M2, AVG decreases smoothly and F95 increases smoothly with increasing vapour quality. No sudden change in the trend appears in the transition zone from intermittent flow to annular flow. The feature space of AVG, M2 and F95 is shown in Figure 4. From this plot, it is also clear that finding the slug/intermittent flow transition will be feasible by using M2. But the intermittent/annular flow transition is rather arbitrary due to the smoothness of this transition.

The choice of the features can be related to the two-phase flows as follows: AVG is a matter for void fraction, M2 is directly related to the presence of liquid slugs and F95 parameter can track the power spectrum contribution shift towards higher frequencies in the intermittent-annular flow transition.

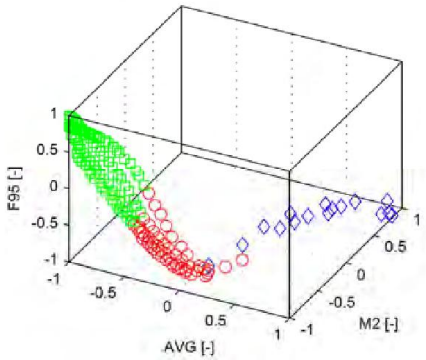

Figure 4 Feature space with our visual classification for R410A (◊ slug flow - o intermittent flow - □ annular flow)

FUZZY C-MEANS CLUSTERING

Clustering algorithms [18] are *unsupervised learning methods*. The goal of such a method is to deduce properties from a dataset, without the help of a supervisor providing correct answers for each observation. It can be applied for two-phase flow classification, without any visual decisions. Clustering analysis tries to group a collection of objects into subsets or clusters such that those within each cluster are more closely related to one another than objects assigned to different clusters. An object is a selection of input features deduced from

a sensor signal. The choice of these input features is fundamental to the clustering technique. The choice of a dissimilarity measure between two objects, the distance function, is a second important factor. By far the most common choice of the distance function is the squared or Euclidian distance.

Each object is iteratively assigned to one cluster based on the minimization of an objective function. Each of the weight parameters can be chosen to set the relative importance of the features upon the degree of similarity of the objects. Variables that are more relevant in separating the clusters should of course be assigned a higher influence in defining object dissimilarity.

The fuzzy c-means clustering algorithm is a *soft-clustering algorithm*. This means that each data point is assigned to a cluster to some degree that is specified by a membership grade *MG*. This allows for describing the boundaries between clusters in a smooth way. Since the aim of the clustering of our datasets is also finding a probabilistic description of flow regime boundaries, this soft-clustering algorithm is the preferred choice amongst other clustering algorithms.

The fuzzy c-means clustering algorithm is applied to the refrigerant flow signal data using a combination of input features which can track both the slug flow/intermittent flow and the intermittent flow/annular flow transition: i.e. the feature input matrix $I = w \cdot [AVG, M2, F95]$. $w_k = 1/(2var_k)$ represents the weight parameters listed in Table 1. By using these values every feature equally contributes to the clustering [18].

Table 1 Variances and weight parameters by feature (after normalization)

	R410A		R134a	
Feature k	var_k	w_k	var_k	w_k
AVG	0.214	2.33	0.269	1.86
M2	0.216	2.31	0.168	2.98
F95	0.415	1.21	0.412	1.21

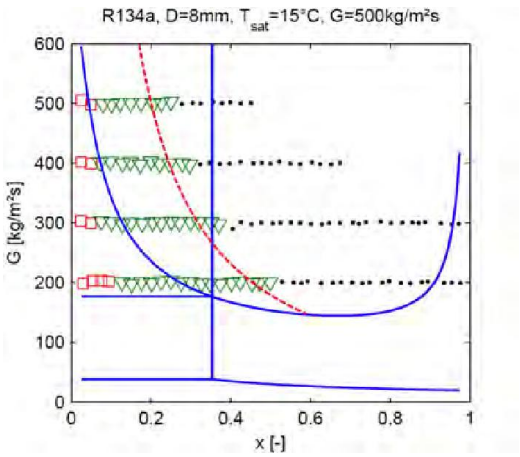

Figure 5 Cluster classification with I = w· [AVG, M2, F95] (symbols are clusters) in a Wojtan-Ursenbacher-Thome flow pattern map [13] (—) and Barbieri et al. [14] intermittent-annular flow transition (---)

The result of using these features to cluster the dataset into three clusters is shown in Figure 5 for R134a. (The results for R410A are very similar). The clustering groups the data points in perfectly separable areas in the flow map. Compared to our visual classification (Figure 2) an excellent agreement is found. The corresponding membership grades are depicted in Figure 6. The membership grades are consistent with the probabilistic flow regime approach and can be interpreted as flow regime probabilities *P*.

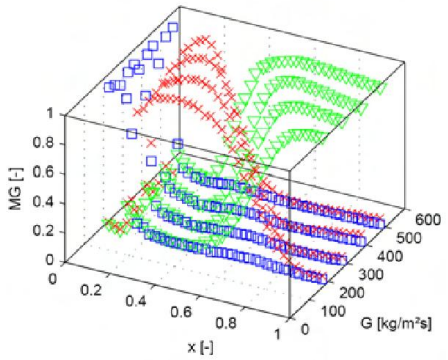

Figure 6 Membership grades (MG) of the cluster algorithm R410A (x slug flow – □ intermittent flow – ∇ annular flow)

PROBABILISTIC FLOW PATTERN MAPPING

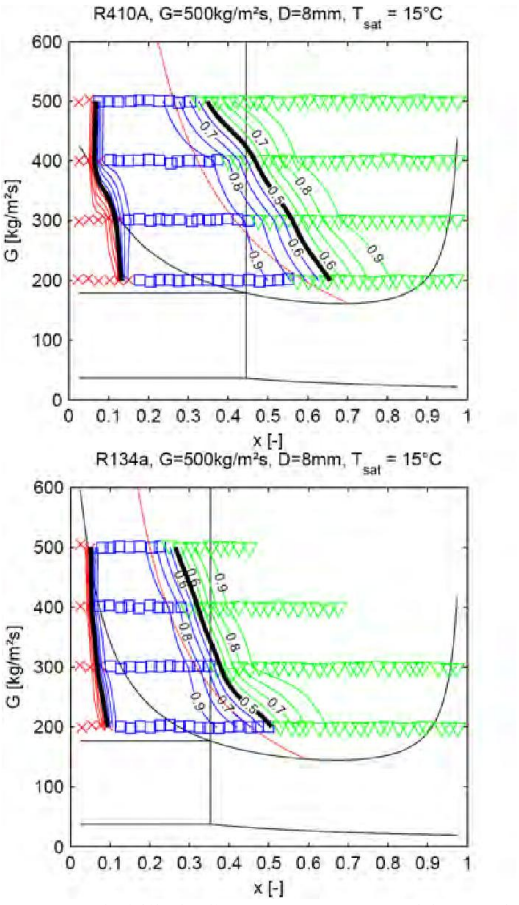

Figure 7 Probabilistic flow pattern maps with our visual classification (x slug flow, □ intermittent flow, ∇ annular flow)

In Figure 7, the probabilistic flow maps are presented for adiabatic flow of R410A and R134a at T_{sat}= 15°C in a horizontal smooth tube of 8mm I.D. at mass velocities ranging from 200 to 500 kg/m^{2}s and vapour qualities from 0 to 1. The flow regime probabilities P are shown as contour lines in the flow map. The 50% probabilities are drawn in black.

It is very clear that the slug flow/intermittent flow transition is a narrow transition zone in the flow pattern map. This is now quantified in terms of the probabilities. The contour lines indicate a width of approximately Δx=0.05. The intermittent/annular flow transition instead is very gradual with a width of over Δx=0.25.

These flow regime probabilities are solely based on the capacitive void fraction signals. The void fraction variations of the two-phase flows are therefore explicitly used in these probabilistic flow pattern maps. Using these flow regime probabilities will assure a proper weighing of the flow phenomena and result in smooth transitions. This can be used for probabilistic heat transfer modelling for evaporating flows.

CONCLUSIONS

A capacitance probe and transducer was developed for use with HFC refrigerants. Sensor signals are gathered with R410A and R134a in an 8mm I.D. smooth tube in the mass velocity range of 200 to 500kg/m²s and vapour quality range from 0 to 1 in steps of 0.025. A visual classification based on high speed camera images is made for comparison reasons. This visual classification confirmed the new intermittent/annular flow transition criterion of Barbieri et al. [14] for use with R410A and T_{sat}=15°C.

The signal average, the variance and a frequency contribution parameter are found suitable for flow regime classification into slug flow, intermittent flow and annular flow. The use of the c-means fuzzy clustering algorithm is investigated for objective flow regime classification purposes. The clustering in feature space groups the data points in clearly separable areas in a flow pattern map. The slug flows could be easily separated from non-slug flows by using the variance of the sensor signal. The AVG and the F95 parameter were found most suitable for separating intermittent flows from annular flows. But, because of the gradual nature of this transition, the choice of this parameter is rather arbitrary.

The soft-clustering algorithm assigns a membership grade to each data point which can be interpreted as a flow regime probability. After regression of these membership grades, flow regimes probability functions were given and probabilistic flow pattern maps were presented for the HFC data. These maps clearly quantify the width of the transition zones and can be applied for probabilistic heat transfer and/or pressure drop modeling.

ACKNOWLEDGMENTS

The authors would like to express gratitude to the BOF fund (B/06634) of the Ghent University - UGent which provided support for this study and thank ir. L. Colman (Vakgroep Electronica, Departement Toegepaste Ingenieurswetenschappen, Hogeschool Gent, Belgium) and ir. G. Colman (Intec_Design, Department of Information Technology, Ghent University, Belgium) for the development of the capacitance transducer.

REFERENCES

[1] Liebenberg, L. and Meyer, J.P., A review of flow pattern-based predictive correlations during refrigerant condensation in horizontally smooth and enhanced tubes, *Heat Transfer Engineering*, Vol. 29, 2008, pp. 3-19

[2] Cheng, L.X., Ribatski, G. and Thome, J.R., Two-phase flow patterns and flow-pattern maps: Fundamentals and applications, *Applied Mechanics Reviews*, Vol. 61, 2008, pp. 050802:1-28

[3] Nino, V.G., Hrnjak, P.S. and Newell, T.A., Two-phase flow visualization of R134A in a multiport microchannel tube, *Heat Transfer Engineering*, Vol. 24, 2003, pp. 41-52

[4] Jassim, E.W., Newell, T.A. and Chato, J.C., Probabilistic determination of two-phase flow regimes in horizontal tubes utilizing an automated image recognition technique, *Experiments in Fluids*, Vol. 42, 2007, pp. 563-573

[5] Jassim, E.W., Probabilistic flow regime modelling of two-phase flow, *PhD thesis*, University of Illinois, Urbana-Champaign, IL, USA, 2006

[6] Jassim, E.W., Newell, T.A. and Chato, J.C., Prediction of refrigerant void fraction in horizontal tubes using probabilistic flow regime maps, *Experimental Thermal and Fluid Science*, Vol. 32, 2008, pp. 1141-1155

[7] Jassim, E.W., Newell, T.A. and Chato, J.C., Prediction of two-phase condensation in horizontal tubes using probabilistic flow regime maps, *International Journal of Heat and Mass Transfer*, Vol. 51, 2008, pp. 485-496

[8] Canière, H., T'Joen, C., Willockx, A., De Paepe, M., Christians, M., van Rooyen, E., Liebenberg, L. and Meyer, J.P., Horizontal two-phase flow characterization for small diameter tubes with a capacitance sensor, *Measurement Science & Technology*, Vol. 18, 2007, pp. 2898-2906

[9] Canière, H., T'Joen, C., Willockx, A. and De Paepe, M., Capacitance signal analysis of horizontal two-phase flow in a small diameter tube, *Experimental Thermal and Fluid Science*, Vol. 32, 2008, pp. 892-904

[10] Colman, G., Canière, H., Colman, L. and De Paepe, M., Fast response capacitance transducer for online measurements of low dielectric fluid two-phase flow, *IEEE Transactions on Instrumentation and Measurement* (under review)

[11] Canière, H., Bauwens, B., T'Joen, C. and De Paepe, M., Probabilistic mapping of adiabatic horizontal two-phase flow by capacitance signal feature clustering, *International Journal of Multiphase Flow*, Vol. 35, 2009, pp. 650-660

[12] Canière, H., Flow pattern mapping of horizontal evaporating refrigerant flow based ond capacitive void fraction measurements, *PhD thesis*, Ghent University - UGent, Gent, Belgium, 2009

[13] Wojtan, L., Ursenbacher, T. and Thome, J.R., Investigation of flow boiling in horizontal tubes: Part I - A new diabatic two-phase flow pattern map, *International Journal of Heat and Mass Transfer*, Vol. 48, 2005, pp. 2955-2969

[14] Barbieri, P., Jabardo, J. and Bandarra Filho, E., Flow patterns in convective boiling of refrigerant R-134a in smooth tubes of several diameters, *5th European Thermal-Sciences Conference*, The Netherlands, 2008

[15] Drahos, J. and Cermak, J., Diagnostics of Gas-Liquid Flow Patterns in Chemical-Engineering Systems, *Chemical Engineering and Processing*, Vol. 26, 1989, pp. 147-164

[16] Shawe-Taylor, J. and Cristianini, N. (2004). "Kernel methods for pattern analysis." *Cambridge University Press*, Cambridge, UK

[17] Jolliffe, I.T. (2002). "Principal Component Analysis." 2nd ed. *Springer*

[18] Bezdek, J.C. (1981). "Pattern Recognition with Fuzzy Objective Function Algorithms." *Plenum Press*, New York, USA